Scleral Cross-Linking in Form-Deprivation Myopic Guinea Pig Eyes Leads to Glaucomatous Changes

Lei Guo,[1,5] Rui Hua,[2] Xinxin Zhang,[1] Ting Yu Yan,[3] Yang Tong,[4] Xin Zhao,[4] Shi Chao Chen,[4] Moying Wang,[1] Neil M. Bressler,[6] and Jun Kong[1]

[1]Department of Ophthalmology, the Fourth Hospital of China Medical University, Shenyang, China
[2]Department of Ophthalmology, the First Hospital of China Medical University, Shenyang, China
[3]Department of Ophthalmology, the Fourth People's Hospital of Shenyang, Shenyang, China
[4]Ocular Pharmacology Laboratory, Shenyang Xingqi Eye Hospital, Shenyang, China
[5]Ophthalmology and Optometry Center, the First Hospital of China Medical University, Shenyang, China
[6]Retina Division, Wilmer Eye Institute, Johns Hopkins University School of Medicine, Baltimore, Maryland, United States

Correspondence: Jun Kong, Department of Ophthalmology, the Fourth Hospital of China Medical University, 11 Xinhua Road, Heping District, Shenyang 110005, Liaoning Province, China; kongjun@hotmail.com.

LG and RH are joint first authors.

Received: July 15, 2021
Accepted: March 6, 2022
Published: May 20, 2022

Citation: Guo L, Hua R, Zhang X, et al. Scleral cross-linking in form-deprivation myopic guinea pig eyes leads to glaucomatous changes. *Invest Ophthalmol Vis Sci.* 2022;63(5):24. https://doi.org/10.1167/iovs.63.5.24

Purpose. To investigate the potential glaucomatous changes caused by scleral cross-linking (CXL) in a guinea pig form-deprivation (FD) myopia model.

Methods. Eighty 4-week-old tricolor guinea pigs were divided into four groups: FD only, genipin CXL only, FD plus CXL, and control. Refractive error, axial length (AL), intraocular pressure (IOP), and structural and vasculature optic disc changes in optical coherence tomography (OCT) and OCT angiography (OCTA) were measured at baseline and day 21. CXL efficacy was evaluated by scleral rigidity Young's modulus values. Histological and molecular changes in the anterior chamber angle, retina, and sclera were assessed.

Results. Baseline parameters were similar among groups ($P > 0.05$). The FD plus CXL group at day 21 had the least increase of AL (0.14 ± 0.08 mm) and highest IOP elevation (31.5 ± 3.6 mmHg) compared with the FD-only group (AL: 0.68 ± 0.17 mm; IOP: 22.2 ± 2.6 mmHg) and the control group (AL: 0.24 ± 0.09 mm; IOP: 17.4 ± 1.8 mmHg) (all $P < 0.001$). OCT and OCTA parameters of the optic disc in the FD plus CXL group at day 21 showed glaucomatous changes and decreased blood flow signals. Sclera rigidity increased in the CXL and FD plus CXL groups. Advanced glycation end products deposited extensively in the retina, choroid, and sclera of FD plus CXL eyes.

Conclusions. CXL causes increased IOP and subsequent optic disc, anterior segment, and scleral changes while inhibiting myopic progression and axial elongation in FD guinea pig eyes. Therefore, applying CXL to control myopia raises safety concerns.

Keywords: deprivation myopia, intraocular pressure, optical coherence tomography, glaucoma, scleral cross-linking, genipin

Myopia has emerged as a major public health issue in east and southeast Asia, with a prevalence of 80% to 90% in young adults, which seems to be related to intensive educational burden and limited outdoor activity.[1] Myopia is caused by excessive elongation of the eye depending on genetically and/or visual experience-based scleral changes, including reduced collagen synthesis, altered collagen fibers and proteoglycans, and increased matrix metalloproteinase activity. Myopic eyes have less sclera thickness and diminished elastic modulus; thus, they become more susceptible to intraocular pressure.[2,3] Interventions to control myopia development and progression include increasing time outdoors, use of low-dose atropine, and orthokeratology. However, none of these interventions prevents continued expansion of the sclera in both children and adults with pathological myopia. Scleral reinforcement or strengthening to restrict scleral expansion may inhibit ocular axial elongation and myopic progression. This theory underlies myopia–posterior scleral reinforcement surgery, which is the only clinically available treatment for pathological myopia.[4,5] However, the safety and the effectiveness of this surgery are controversial.[6]

In recent years, scleral cross-linking (CXL) has been performed to prevent ocular axial elongation in form-deprivation (FD) myopic guinea pigs, a classical animal model of myopia, and other animal models. CXL is similar to posterior sclera reinforcement surgery in principle. The CXL method enhances scleral biomechanical strength, inhibiting the growth of form-deprivation myopia (FDM).[7–9] Both physical and chemical CXL methods strengthen scleral biomechanical rigidity without obvious side-effects; therefore, it has been suggested that scleral CXL may be a promising method to control pathological myopia progression. However, there is a concern that CXL may increase the risk of glaucoma, as suggested by increased intraocular pressure (IOP) and more susceptible retinal ganglion cells damage to IOP fluctuation in mice eyes.[10] Moreover, an increased corneoscleral stiffness may significantly increase IOP spike magnitudes at the same volumetric change.[11] Most importantly, although few studies investigated the potential risks

of scleral CXL in animal models, to our knowledge, none has systemically studied the potential changes in FD plus scleral CXL myopic eyes.[12] As we already know, myopic eyes are more vulnerable and susceptible to IOP. Therefore, to gain insight into the safety of this treatment for myopia, it is important to investigate if IOP fluctuation, morphological optic disc changes, and pathophysiological anterior chamber changes occur after scleral CXL in myopic eyes.

In this study, we investigated the changes of ocular axial length (AL), refraction, IOP, and optical coherence tomography (OCT) parameter of the optic disc in FDM guinea pigs with and without sub-Tenon's injection of the CXL agent genipin. We also investigated the effect thereof on several glaucoma-related biomarkers in the sclera, aqueous humor, and anterior chamber angle at histological and molecular levels.

Materials and Methods

FD Myopia Animal Model

The right eyes of 80 4-week-old tricolor guinea pigs, weighing 200 to 240 g, were selected as the study eyes. Animals with congenital cataract, corneal abnormalities, or other ocular diseases that may affect vision were excluded at baseline. All animal care and treatment in this study conformed to the ARVO Statement for the Use of Animals in Ophthalmic and Vision Research, and all experimental protocols were approved by the Animal Care and Use Committee of China Medical University. Guinea pigs were randomly divided into four groups according to the intervention: FD only ($n = 20$), CXL only ($n = 20$), FD plus CXL ($n = 20$), and control ($n = 20$). An FDM model was established according to Wang et al.[7] (Fig. 1).

To achieve FD, latex balloons (OuJie CO., LTD, Suzhou, China) were modified into facemasks that covered only the right eye of each animal for 3 weeks, leaving the left eye, nose, mouth, and ears exposed. The facemask was made of soft, translucent elastic latex (6%–8% light transmission as measured by the Humphrey Field Analyzer; Carl Zeiss Meditec, Jena, Germany) with an average thickness of 0.02 ± 0.01 mm. The facemask did not stretch, compress, or restrict blink movements of the form-deprivation eyes, and it could be easily applied, negating the need for anesthesia for this procedure. The eye mask was replaced with a new one daily in a semi-dark room.

Genipin Scleral CXL Procedure

Sub-Tenon's injection (29-gauge needle) of 0.10 mL of 0.50% genipin (FUJIFILM Wako Pure Chemical Industries, Osaka, Japan) in saline was administered at 3.0 mm behind the limbus in both the inferonasal and superotemporal quadrants of the CXL-only eyes and FD plus CXL eyes (Fig. 1). A small-incision squint hook was used to spread the genipin solution to the back of the eyeball to ensure extensive CXL of the sclera. All injections were administered under light general anesthesia (intraperitoneal injection of 1% pentobarbital sodium, 0.33 mL/100 g). The first injection was administered at day 0 (4 weeks old) and was repeated twice more at 7-day intervals. In the control group, a sub-Tenon's injection of 0.10 mL of saline was administered at 3.0 mm behind the limbus in both the inferonasal and superotemporal quadrants of the right eye with the same strategy. After the procedure, daily antibiotic eye drops (Levofloxacin; Shenyang Sinqi Pharmaceutical Co., Ltd., Shenyang, China) were applied for 3 days.

In Vivo Parameter Measurements

The following measurements were performed at baseline and at specified intervals: Refractive error was measured by streak retinoscope (YZ-24 Streak Retinoscope; Suzhou Liuliu Vision Technology, Suzhou, China) at days 0 and 21. IOP was measured using a TonoLab tonometer (iCare, Vantaa, Finland) according to the manufacturer's recommended procedures at days 0, 7, 14, and 21. Ocular AL was measured by manual mode of A-mode ultrasound (Aviso; Quantel Medical, Inc., France) at days 0 and 21. Guinea pig IOP also exhibits diurnal variation, peaking in the early morning (mean of 25.8 mmHg at ~9 AM) and decreasing throughout the day.[13] Measurements were performed around a fixed time each day (9:00 AM–12:00 PM) to avoid the confounding effects of diurnal rhythms. IOP measurements in FD eyes showed stable progression from high to low after removal of the masks. Therefore, 5 seconds after removal of the blindfold, awake guinea pigs were gently restrained by hand while three sets of six tonometer readings were recorded.

The optic disc was measured by spectral domain OCT (Cirrus HD-OCT 5000; Carl Zeiss Meditec) and OCT angiography (OCTA) (Fig. 1) under general anesthesia by injecting 1% luciferin sodium intraperitoneally at days 0 and 21. The analyzed parameters included morphological changes of the optic disc, average cup-to-disc ratio (CDR), vertical CDR, circumpapillary retinal nerve fiber layer (cpRNFL; µm), disc area (mm^2), rim area (mm^2), and cup volume (mm^3). The changes of blood flow in optic disc were detected by Phoenix MICRON fluorescein angiography (Phoenix-Micron, Bend, OR, USA).

Functional Measurements and In Vitro Experiments

At day 21, guinea pigs were assigned to undergo functional examinations under general anesthesia using pentobarbital

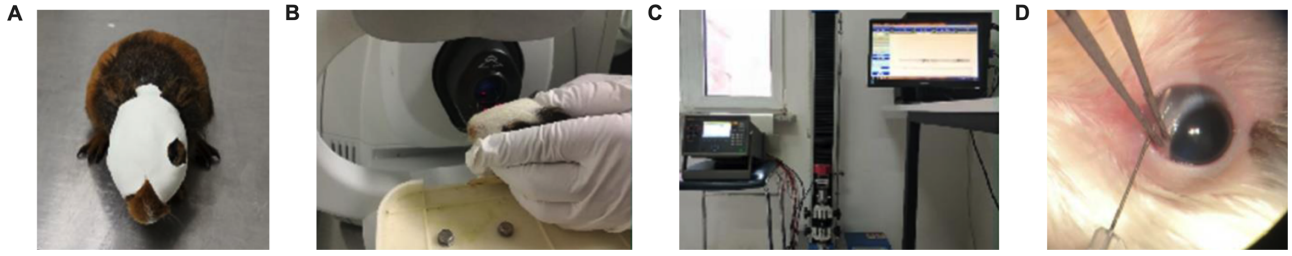

Figure 1. Establishment of animal models and measurements. (**A**) A guinea pig undergoing form deprivation. (**B**) OCT examination based on the animal bracket. (**C**) Equipment for stress–strain measurement of the scleral strip. (**D**) Genipin scleral CXL procedure.

Investigative Ophthalmology & Visual Science

sodium (intraperitoneal [IP] injection, 35 mg/kg) or to be euthanized with an overdose of pentobarbital sodium (IP injection, 150 mg/kg) and enucleated for subsequent experiments. Two micro liter aqueous humor from the right eyes of the FD-only group, CXL-only group, and FD plus CXL group (each group, $n = 5$) was collected. Soluble cluster of differentiation antigen 44 (sCD44) levels in the aqueous humor were determined by enzyme-linked immunosorbent assay (ELISA) kits (NBP2-75154, Novus Biological, Littleton, CO, USA) according to the manufacturer's instructions.

For functional examination of aqueous humor outflow, 5 µm of the conjunctiva and lower fascia tissue were cut off along the cornea to expose the bottom of the sclera and the blood vessels on the scleral surface. One micro liter 0.4% trypan blue solution was injected into the anterior chamber by a 29-gauge needle. Outflow of trypan blue was observed and recorded under microscope.

Measurement of Scleral Rigidity

Biomechanical measurements were performed based on 40 scleral specimens from the four groups ($n = 10$ per group). After removing the external muscles, a scleral strip was dissected at 2 to 7 mm behind the scleral margin from the superonasal to superotemporal region. The retina and choroid were removed using a saline sponge. The strips (10 mm × 5 mm) were immersed into 0.9% saline solution for approximately 2 hours and were then placed on a filter paper for 5 minutes. The thickness of the strips was determined using a mechanical micrometer caliper. The dehydrated strips were placed on a computer tension tester and clamped to ensure that the measurements were taken in the center. Before the formal experiment, a pre-experiment was performed to evaluate the computerized tension tester (Fig. 1). To perform the stress–strain test on the scleral strips, each strip was subjected to five cycles of deformation-load testing. Strain was increased linearly at a velocity of 1 mm/min until tissue rupture. The maximum force (N) and tensile strength (MPa) at rupture were recorded, as well as the deformation level and elongation level (mm) at the ultimate strain. Young's modulus E (MPa) was calculated for the ultimate strain as the gradient of the stress–strain graph ($E = d\sigma/d\varepsilon$).

Histological Examinations

Five enucleated eyeballs from each group (FD only, CXL only, and FD plus CXL) were fixed in 4% paraformaldehyde immediately after euthanasia. After decalcification, paraffin embedding, and sectioning, samples were stained with hematoxylin and eosin (H&E). Another three enucleated eyeballs from each group were fixed in 2% glutaraldehyde for transmission electron microscopy. Thin sections (60–90 nm) were stained with lead citrate and uranyl acetate and examined under a transmission electron microscope (JEM-2100; JEOL Ltd., Tokyo, Japan). Electron micrographs of the collagen fibrils at a magnification of 40,000× were taken from the center bundle of sclera. Twelve 2 × 2-µm fields were photographed from 12 electron micrographs of the three samples in each group.

Immunofluorescence

The retinal, choroidal, and scleral tissues dissected from the enucleated eyes were fixed and embedded with paraffin. Sections were blocked with 5% bovine serum albumin in phosphate-buffered saline for 30 minutes at room temperature. The samples were incubated with primary antibodies to advanced glycation end products (AGEs), matrix metalloproteinase-2 (MMP-2), and tissue inhibitor of matrix metalloproteinase-2 (TIMP-2) overnight at 4°C and incubated with secondary antibodies for 1 hour at room temperature. Controls were included in each experiment without using primary antibodies. Images were captured by an inverted fluorescence microscope (Nikon Eclipse TE 2000-U microscope; Nikon, Tokyo, Japan). Apoptosis was quantified by terminal deoxynucleotidyl transferase-mediated dUTP nick end-labeling (TUNEL) assay. For double staining, nestin immunohistochemistry was conducted followed by green fluorescent protein immunohistochemistry.

Western Blot and Reverse-Transcription Quantitative Polymerase Chain Reaction

Proteins from scleral tissues taken 5 to 7 mm behind the angular scleral margin were extracted and separated by 10% SDS-PAGE and then blotted onto polyvinylidenfluoride (PVDF) membranes. After being blocked in 5% non-fat milk, PVDF membranes were treated with specific primary antibodies overnight at 4°C. Secondary antibodies were subsequently used for incubation. An electrochemiluminescence kit (Thermo Fisher Scientific, Waltham, MA, USA) was applied for visualization of the bands. Total RNA was isolated by TRIzol (Thermo Fisher Scientific) from scleral tissue at 5 to 7 mm behind the angular scleral margin. cDNA was synthetized, and SYBR Green (Thermo Fisher Scientific) was applied for quantitative polymerase chain reaction with cDNA as templates and glyceraldehyde-3-phosphate dehydrogenase (GAPDH) as internal control. Primer sequences were as follows:

MMP-2 forward: 5′-CAGGACATTGTCTTTGATGGCATCGC-3′
MMP-2 reverse: 5′-TGAAGAAGTAGCTATGACCACCGCC-3′
TIMP-2 forward: 5′-GAGCGAGAAGGAGGTGGATTCCGGG-3′
TIMP-2 reverse: 5′ATGTCAAGAAACTCCTGCTTCGGGGG-3′

Statistical Analyses

Data are presented as mean ± SD. Differences in refraction, IOP, AL, scleral rigidity, OCT-based optic disc parameters, and scleral biomechanical parameters at day 21 were compared to those of the baseline using the paired-sample t-test and were compared among the four groups using both t-test and one-way ANOVA with Bonferroni correction. Differences in optic nerve head morphology on three-dimensional (3D) OCT and optic disc blood flow in OCTA were described. All statistical analyses were performed using SPSS Statistics 18.0 (IBM, Chicago, IL, USA). Statistical significance was defined as $P < 0.05$.

Results

FD Myopia Animal Model

Baseline information of the four groups is shown in Table 1. On average, the eyes of 4-week-old guinea pigs had an average AL of 7.39 ± 0.14 mm, average IOP of 17.13 ± 2.10 mmHg, and average refraction power of 2.42 ± 1.20 diopters (D). There were no significant differences in refraction, IOP, AL, and OCT parameters among the four groups at baseline (all $P > 0.05$) (Table 1).

Investigative Ophthalmology & Visual Science

Table 1. General Information and OCT Parameters at Baseline

Group (n = 12 Each)	Refraction (D)	IOP (mmHg)	Axial Length (mm)	Average CDR	Vertical CDR	cpRNFL (μm)	Rim Area (mm^2)	Disc Area (mm^2)	Cup Volume (mm^3)
FD only	2.33 ± 1.25	17.4 ± 2.64	7.39 ± 0.12	0.33 ± 0.99	0.34 ± 0.09	58.6 ± 10.48	0.71 ± 0.09	0.73 ± 0.09	0.03 ± 0.01
CXL only	2.46 ± 0.96	16.8 ± 1.59	7.39 ± 0.10	0.33 ± 0.76	0.33 ± 0.07	58.8 ± 11.66	0.72 ± 0.12	0.74 ± 0.12	0.03 ± 0.01
FD plus CXL	2.78 ± 1.42	17.4 ± 1.98	7.39 ± 0.14	0.34 ± 0.12	0.34 ± 0.13	58.7 ± 7.91	0.71 ± 0.13	0.74 ± 0.14	0.03 ± 0.01
Control	2.50 ± 1.70	16.8 ± 2.25	7.40 ± 0.21	0.33 ± 0.08	0.33 ± 0.08	58.4 ± 12.28	0.70 ± 0.07	0.74 ± 0.09	0.03 ± 0.09
F, P	F = 0.04	F = 0.29	F = 0.01	F = 0.03	F = 0.02	F = 0.00	F = 0.03	F = 0.06	F = 0.02
	P = 0.99	P = 0.83	P = 0.10	P = 0.99	P = 1.00	P = 1.00	P = 1.00	P = 0.98	P = 1.00

All $P > 0.05$.

A

Parameters of Refraction and Axial length

Groups	Refraction (D)			Axial length (mm)		
(Each n = 12)	Baseline	Day 21	t Values, P Values	Baseline	Day 21	t Values, P Values
FD only	2.33 ± 1.25	-2.33 ± 1.25*†	t = 14.5, P < .001	7.39 ± 0.12	8.07 ± 0.15*†	t = 14.04, P < .001
CXL only	2.46 ± 0.96	2.54 ± 1.23	t = 0.46, P = 0.66	7.39 ± 0.10	7.49 ± 0.10*	t = 7.33, P < .001
FD+ CXL	2.38 ± 1.42	1.67 ± 1.29*	t = 3.74, P < .001	7.39 ± 0.14	7.54 ± 0.13*	t = 6.12, P < .001
Control	2.50 ± 1.30	0.92 ± 1.52*	t = 11.70, P < .001	7.40 ± 0.21	7.64 ± 0.22	t = 9.44, P < .001
		F = 30.83, P < .001			F = 34.48, P < .001	

Note: * means the parameters were significantly increased at Day 21 compared with those of the baseline, and † means the parameters was significantly changed than those in the other three groups at Day 21 (P < .001).

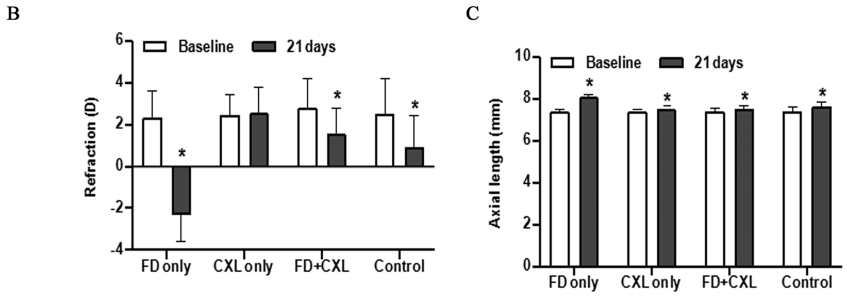

Figure 2. Comparison of refraction and axial lengths between baseline and day 21. (**A**) Parameters of refraction and axial length. (**B**) There were different levels of myopic aggravation of refraction in FD-only eyes, FD plus CXL eyes, and control eyes at day 21. (**C**) Correspondingly, different increases in axial length were demonstrated. *$P < 0.05$.

In Vivo Parameter Measurements

By day 21, AL increased significantly in all four groups (FD-only group: 0.68 ± 0.17 mm; CXL-only group: 0.10 ± 0.05 mm; FD plus CXL group: 0.14 ± 0.08 mm; control group: 0.24 ± 0.09 mm) (all $P < 0.001$). The AL elongation in the FD group was significantly greater than in the other three groups ($F = 76.84$, $P < 0.001$). The two genipin CXL groups had the shortest axial length at day 21 even when compared with the control group (Fig. 2).

At day 21, there were different levels of myopic aggravation of refraction in the FD-only group (−4.67 ± 1.12 D), FD plus CXL group (−0.71 ± 0.66 D), and control group (−1.58 ± 0.47 D). However, no myopic aggravation was found in the CXL-only group (0.08 ± 0.63 D) (Fig. 2), which means the current sclera cross-linking strategy is effective in preventing FDM. The FD-only group had the largest myopic refraction power at day 21 ($F = 90.53$, $P < 0.001$). Refraction power in the FD plus CXL group at day 21 showed no statistically significant differences when compared with either the CXL-only group ($P = 0.113$) or the control group ($P = 0.173$).

IOP was measured at baseline and at days 7, 14, and 21 (Fig. 3). Compared with baseline, IOP at day 21 in the FD-only group (22.2 ± 2.6 mmHg), CXL-only group (23.7 ± 2.5 mmHg), and FD plus CXL group (31.5 ± 3.6 mmHg) increased significantly (all $P < 0.001$). However, IOP in the control group was stable from the baseline (17.7 ± 1.8 mmHg) to day 21 (17.4 ± 1.8 mmHg).

Eyes in the FD plus CXL group at day 21 had the biggest average CDR (0.65 ± 0.06), cpRNFL (67.8 ± 7.3 μm), and cup volume (0.08 ± 0.015 mm^2) and the lowest rim area (0.54 ± 0.1 mm^2) compared with those of the baseline (CDR: 0.34 ± 0.12; cpRNFL: 58.7 ± 7.9 μm; cup volume: 0.03 ± 0.01 mm^2; rim area: 0.71 ± 0.13 mm^2) and the other three groups at day 21 (all $P < 0.001$) (Table 2). Optic disc depression was observed in 3D-OCT in the FD plus CXL group. Additionally, the optic disc flow signal in both OCTA and fluorescein sodium angiography decreased visibly at day 21 compared with baseline in the FD plus CXL group (Fig. 4).

Functional Measurements and In Vitro Experiments

ELISA results showed that sCD44 levels in the aqueous humor were significantly higher in the FD-only group

Investigative Ophthalmology & Visual Science

A

Intraocular Pressure Changes of Each Group ($\bar{X}$ ± SD)

	FD (mmHg)	CXL (mmHg)	FD + CXL (mmHg)	Control (mmHg)
Baseline	17.4 ± 2.64	16.8 ± 1.59	17.4 ± 1.98	16.8 ± 2.25
7 days	18.7 ± 2.10	19.8 ± 1.71	22.9 ± 2.19	17.3 ± 2.18
14 days	21.2 ± 2.17	22.1 ± 1.83	27.9 ± 2.15	17.3 ± 2.18
21 days	22.2 ± 2.59	24.2 ± 1.99	31.5 ± 3.56	17.1 ± 1.78

Two-way ANOVA results of Intraocular Pressure

Source of Variation	Df	Sum-of-squares	Mean square	F ratio	P value
Interaction	9	678.9	75.44	27.80	< .0001
Time	3	1204	401.5	147.9	< .0001
Column Factor	3	1509	503.1	43.54	< .0001
Subjects (matching)	44	508.5	11.56	4.258	< .0001
Residual	132	358.2	2.714		
Total	191	4259			

B

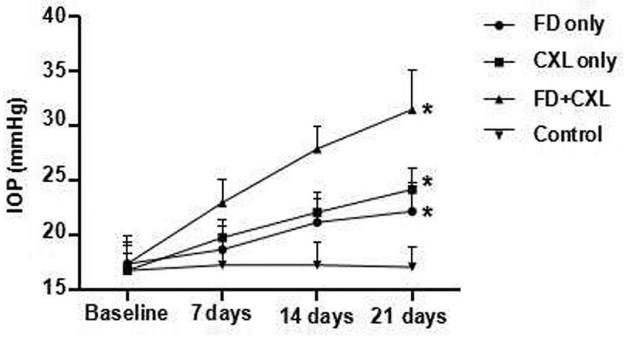

Figure 3. (**A**) IOP changes of each group and two-way ANOVA results for IOP. (**B**) The changes in IOP among the four groups over 21-day follow-up. IOP in FD-only eyes, CXL-only eyes, and FD plus CXL eyes increased significantly compared with the baseline ($P < 0.05$).

Table 2. OCT Parameters of Optic Disc at Day 21

Group ($n = 12$ Each)	Average CDR	Vertical CDR	cpRNFL (μm)	Rim Area (mm^2)	Disc Area (mm^2)	Cup Volume (mm^3)
FD only	0.35 ± 0.11*	0.36 ± 0.11	58.8 ± 14.2	0.71 ± 0.11	0.76 ± 0.08	0.03 ± 0.012*
CXL only	0.36 ± 0.13	0.38 ± 0.13	65.3 ± 12.5*	0.65 ± 0.12	0.75 ± 0.12	0.04 ± 0.010*
FD plus CXL	0.65 ± 0.06*†	0.63 ± 0.06*†	67.8 ± 7.3*	0.54 ± 0.10*†	0.82 ± 0.16*	0.08 ± 0.015*†
Control	0.34 ± 0.06	0.34 ± 0.08	58.9 ± 10.5	0.71 ± 0.08	0.76 ± 0.10	0.031 ± 0.009
F, *P*	$F = 29.52$	$F = 21.45$	$F = 1.92$	$F = 7.89$	$F = 0.96$	$F = 37.95$
	$P < 0.001$	$P < 0.001$	$P = 0.14$	$P < 0.001$	$P = 0.42$	$P < 0.001$

* Parameters were significantly increased at day 21 compared with those of the baseline.
† Parameters were significantly larger than those in the other three groups at day 21 ($P < 0.001$).

and FD plus CXL group than in the control group. The increment in FD plus CXL group was significantly higher ($P < 0.05$) (Fig. 5). Slight corneal edema and elevated IOP were observed by microscopy after 0.2 μL of 0.4% trypan blue solution was injected into the anterior chamber. Five minutes after injection, blue staining of veins at limbus was observed in the normal control group, and a delayed staining at 7 minutes after injection was observed in the FD plus CXL group. The filling duration of trypan blue in the super scleral vein in the FD plus CXL group was shorter than in the control group (Fig. 6). However, no atresia or stenosis was observed in the vorticity vein in the eyes of the FD plus CXL group (Fig. 6).

Investigative Ophthalmology & Visual Science

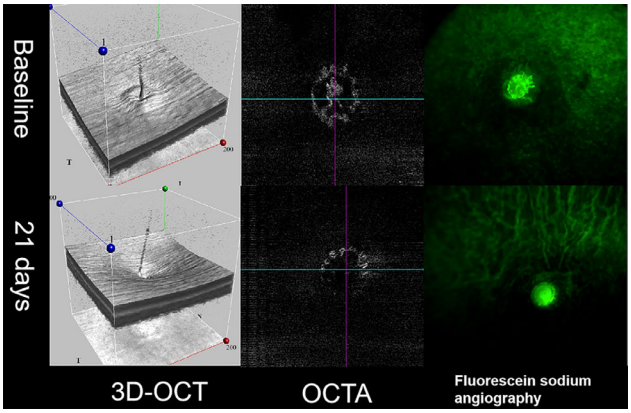

Figure 4. The angiographic and morphologic characteristics of the optic disc in FD plus CXL eyes. Compared with baseline, depression of the optic disc in FD plus CXL eyes at day 21 was observed in 3D-OCT, as well as reduced blood flow signal in both OCTA and fluorescein sodium angiography.

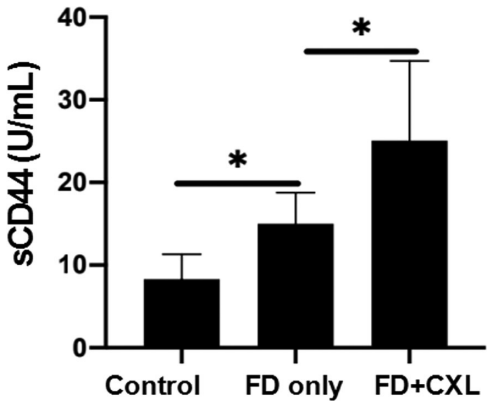

Figure 5. After 3-week intervention, the sCD44 levels in the aqueous humor of FD-only eyes and FD plus CXL eyes were significantly higher than for the control eyes. The increments were more obvious in FD plus CXL eyes than in FD-only eyes ($P < 0.05$).

Measurement of Scleral Rigidity

Compared with the other three groups, the FD group had the lowest Young's modulus, highest deformation at the maximum force point, and the maximum elongation rate at day 21 (all $P < 0.05$). In contrast, there was a statistically significant increment in the biomechanical parameters of the CXL eyes in the CXL-only group and FD plus CXL group compared with the FD and control groups (all $P < 0.001$) (Table 3).

Histological Examinations

Under light microscopy, the anterior chamber angles of eyes in the FD group and FD plus CXL group were open, and no obvious adhesion of the trabecular meshwork and extracellular matrix was observed. In the FD-only eyes, the sclera thinned significantly, and fewer vessels were observed in the choroidal layers. In contrast, thicker choroid was observed in the FD plus CXL eyes, and there was no apparent vessel density deduction in the choroid (Fig. 7). The scleral collagen fibers in FD-only eyes were scattered and irregularly distributed in electron micrographs. The scleral collagen fibers in CXL-only, FD plus CXL, and control eyes were more regularly distributed and denser than those in FD-only eyes (Fig. 8).

Expression of MMP-2, TIMP-2, and AGEs

At day 21, paraffin sections showed that AGEs were deposited extensively in the retina, choroid, and sclera of the FD plus CXL eyes and were less obviously deposited in the sclera of the FD-only eyes (Fig. 9). There was almost no AGE deposition in control eyes. Western blots showed that MMP-2 and TIMP-2 expression in the scleral tissues was increased in the FD-only group and FD plus CXL group, as compared with the control group. MMP-2 expression was increased more markedly than TIMP-2 expression in FD-only eyes, and TIMP-2 was increased more markedly than MMP-2 in FD plus CXL eyes. The same trends were confirmed by the reverse-transcription PCR and immunofluorescence (Fig. 10).

Discussion

In this study, axial myopia was induced after FD in guinea pig eyes. A significant increase in IOP after CXL was observed in the FD myopic eyes. Sub-Tenon's injection using 0.50% genipin solution effectively increased scleral hardness and inhibited the development of FDM in the guinea pigs, consistent with previous reports.[7–9,14–16] However, we showed that experimental alteration of scleral rigidity in FD guinea pig eyes can increase IOP and cause glaucomatous changes in the optic disc and sclera at a histological and molecular level, which has not been reported previously.

Figure 6. Five minutes after injection, blue staining of veins at limbus was observed in the control eyes, and a delayed staining at 7 minutes after injection was observed in FD plus CXL eyes. The filling times of 0.4% trypan blue in super scleral veins in FD plus CXL eyes were shorter than in the normal control eyes.

Investigative Ophthalmology & Visual Science

Table 3. Thickness and Biomechanical Properties of Sclera in Each Group at Day 21

Groups (n = 10 Each)	Maximum Force (N)	Ultimate Stress (MPa)	Maximum Elongation Rate (%)	Young's Modulus (MPa)	Scleral Area (mm^2)	Scleral Thickness (μm)	Scale Distance (mm)
FD only	1.40 ± 0.10*	5.97 ± 0.35*	20.03 ± 2.33*	30.15 ± 3.75*	0.23 ± 0.00	57 ± 1	5
CXL only	2.46 ± 0.38*	9.95 ± 0.98*	14.85 ± 1.69	67.87 ± 10.94*	0.23 ± 0.00	57 ± 1	5
FD+CXL	2.27 ± 0.16*	9.70 ± 0.55*	14.98 ± 1.18	65.17 ± 6.83*	0.23 ± 0.00	56 ± 2	5
Control	1.77 ± 0.27	7.58 ± 0.81	17.06 ± 1.91	44.71 ± 4.93	0.23 ± 0.00	56 ± 2	5
F, P	F = 37.50 P < 0.001	F = 69.36 P < 0.001	F = 11.67 P < 0.001	F = 62.26 P < 0.001	F = 0.09 P = 0.967	F = 1.26 P = 0.303	—

Sclera in the CXL and FD plus CXL groups had similar maximum force values (P = 0.096), which were significantly higher than those of FD-only eyes and control eyes. All P < 0.001.

* Parameters were statistically different compared to the control group (P < 0.001).

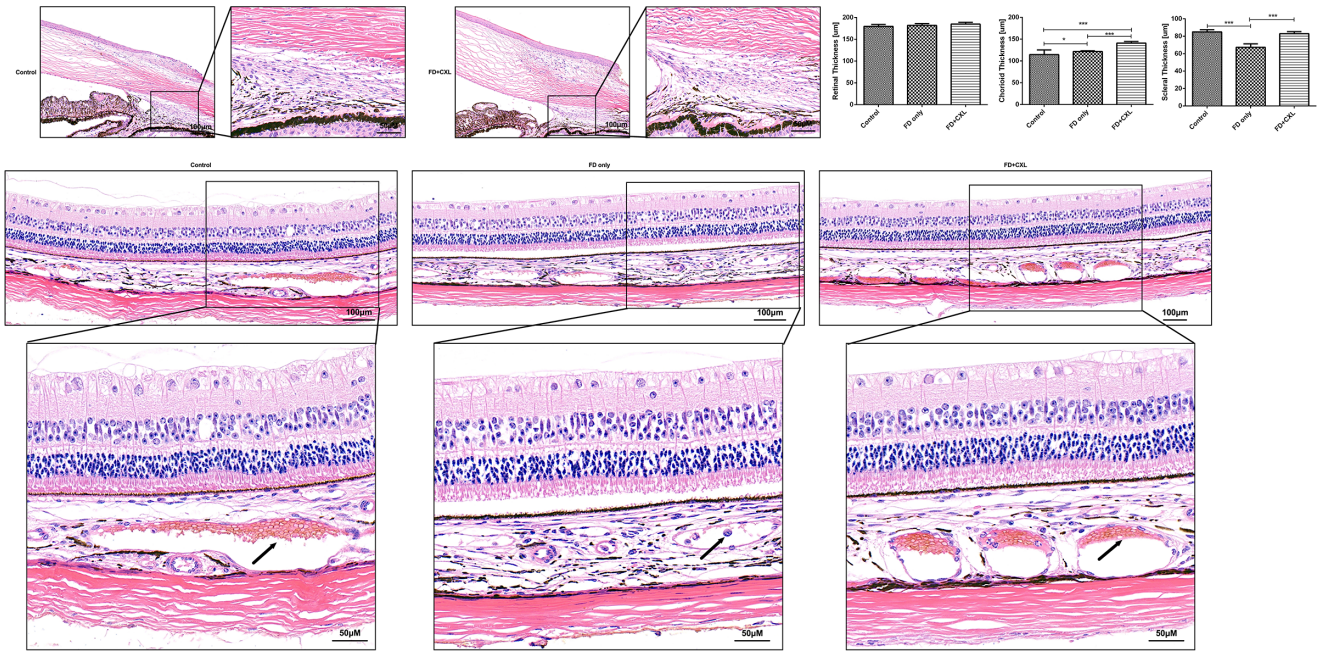

Figure 7. Under a light microscope, there was no obvious narrowing of the chamber angle in FD-only eyes and FD plus CXL eyes at day 21. H&E staining showed attenuated blood vessels in the choroid and thinned sclera in the FD eyes versus normal blood vessels and thicker sclera in the FD plus CXL eyes.

Our data showed that IOP increased either by FD alone or CXL alone in guinea pig eyes in a time-dependent manner. Combining FD and CXL caused significant further IOP elevation than for FD alone or CXL alone. At day 21, the optic discs of the FD plus CXL guinea pig eyes showed morphological changes similar to those of human glaucomatous optic discs on OCT, as demonstrated by increased mean and vertical CDR, narrowing of the optic disc margin, and significantly increased cup volume. In 3D-OCT graphics, characteristic glaucomatous changes were shown in the FD plus CXL eyes, including reduced or disappeared ring uplift in the lithosphere, increased cup volume, and deepened optic disc depression. These manifestations are similar to the clinical reports of glaucoma in human eyes.[17–19]

Although many studies have demonstrated the efficacy of scleral CXL in blocking FDM in animal models, to our knowledge none has systemically studied the potential changes that may be similar to or consistent with glaucoma. Most of these studies did not measure IOP, nor did they measure optic disc or histological changes after scleral CXL. OCT facilitates imaging and studying of the optic disc in animal models.[20–22] Few studies have employed 3D imaging of the optic disc or OCTA technology to study the details of vessels around optic discs in animal models. Our study showed that the optic disc blood flow was significantly reduced in optic disc angiography performed by Phoenix OCTA in the FD plus CXL eyes at day 21.

In this study, the mechanism underlying glaucomatous changes in the optic disc of FD plus CXL eyes was considered to be mainly related to the increased scleral thickness induced by CXL. Scleral stiffness is related not only to myopia development but also to high IOP and glaucoma.[23–26] IOP may be one of the factors that promote passive dilation in myopic eyes,[1] which has been confirmed in animal experiments of FDM.[27] IOP elevation can lead to nonlinear deformation of the sclera. Scleral expansion can relieve the impact of the pressure on the lamina.[27–33] Creep deformation occurs as the IOP continues to increase.[34–37] The mechanical behavior of the sclera significantly affects the stress and deformation of the lamina,

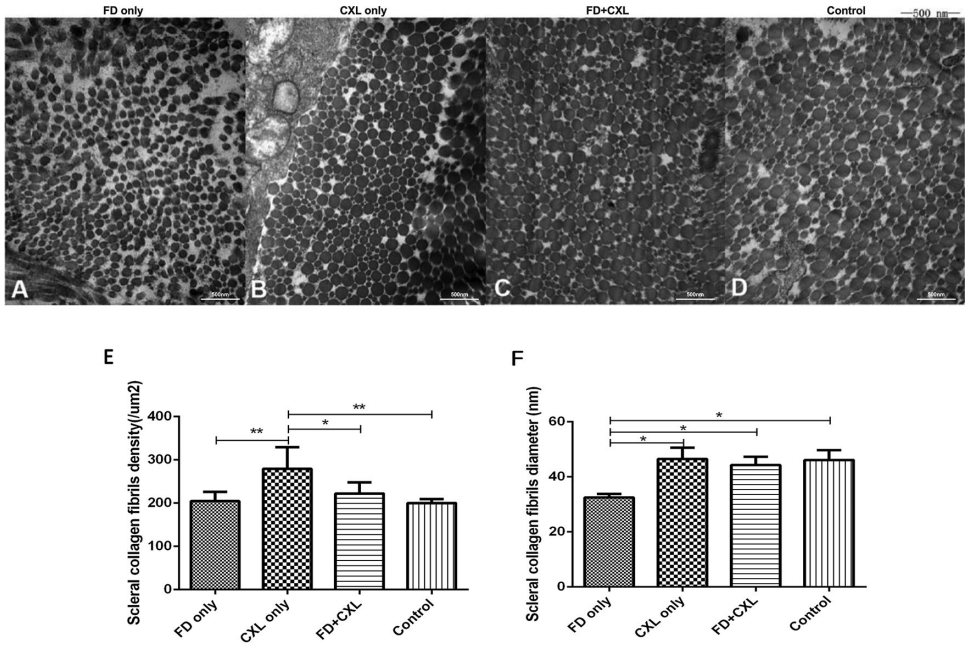

Figure 8. Electron micrographs of the guinea pig sclera. (**A**) Scattered and irregularly distributed scleral collagen fibrils in the FD myopic eyes at day 21 (original magnification, 40,000×). (**B**) Dense scleral collagen in CXL-only eyes. (**C**) Scleral collagen in FD plus CXL eyes. (**D**) Scleral collagen fibrils in control eyes. (**E**) Scleral collagen fibril density. (**F**) Scleral collagen fibril diameter. *$P < 0.05$; ** $P < 0.01$.

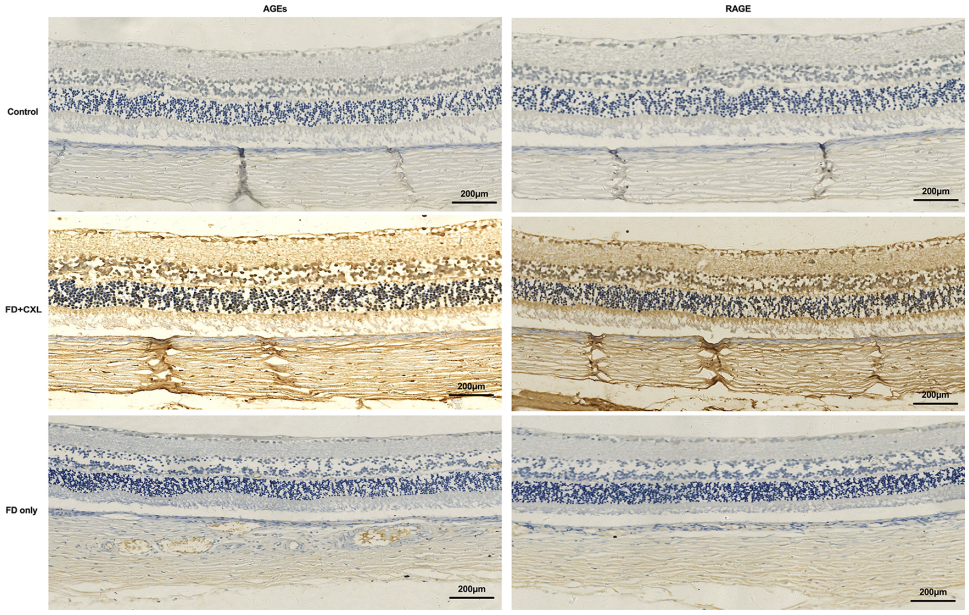

Figure 9. Advanced glycation end products were deposited in the retina, choroid, and sclera of FD plus CXL eyes and in the sclera of FD-only eyes. The difference was significant compared with the control group ($P < 0.05$).

which is probably a key mechanical driving factor of glaucomatous damage to the axons of the retinal ganglion cells.[38,39,40] Some studies have demonstrated that scleral stiffening, as observed in human glaucoma eyes, is not a beneficial adaption but is a detrimental contributor to optic nerve head injury.[26,36] CXL causes increased scleral stiffness and reduced deformation ability, as well as eye elongation. Kimball et al.[10] reported that scleral CXL could increase susceptibility to retinal ganglion cell (RGC) damage in mice. They injected glyceraldehyde subconjunctivally in mice without FD, then induced a glaucoma model by injecting beads into the anterior chamber. Although the study suggested that glyceraldehyde-treated mouse eyes had greater RGC axon loss due to the elevated IOP induced by the bead injection, glyceraldehyde exposure alone did not affect the RGC number, or retinal structure or function. Hannon et al.[12] performed one-time injection of 150 µL of 15-mM genipin in non-myopic Brown Norway rat eyes.

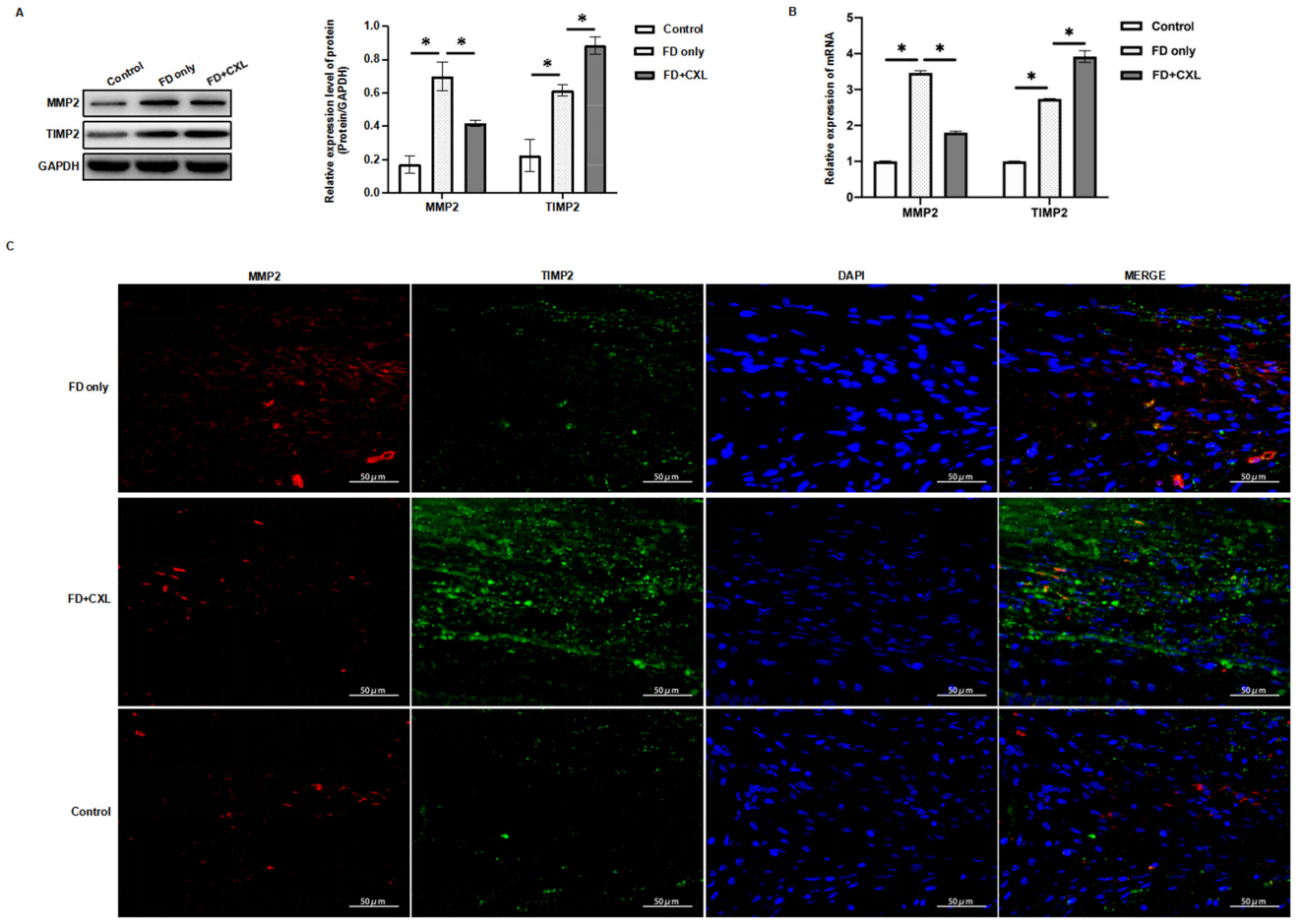

Figure 10. The expression levels of MMP-2 and TIMP-2 in both the sclera and trabecular meshwork increased in FD and FD plus CXL eyes. In FD eyes, MMP-2 expression increased markedly compared with TIMP-2 expression. After scleral CXL, the increment of TIMP-2 expression was more obvious than that of MMP-2.

There was no impact on IOP or retinal function, nor was there a sustained impact on visual function, although there was a non-statistically significant axonal loss (9.4% ± 23.8%) in genipin-injected eyes compared to fellow control eyes. However, these studies did not clarify whether scleral stiffening could cause glaucoma or glaucomatous changes in compromised myopic eyes, which are more susceptible to IOP compared to none myopic eyes. Our study demonstrated that in FD guinea pig eyes, although the increased scleral stiffness by CXL can prevent or reduce myopic changes, it could also cause glaucomatous changes in the optic disc. Features of glaucomatous changes appeared at 3 weeks after FD plus CXL treatment in guinea pig eyes, which were further demonstrated by the increased expression of glaucoma-related markers at a molecular biological level. In our study, although no significant apoptosis of RGCs was observed in the FD plus CXL eyes, AGEs, which are a typical neurodegenerative marker,[41–43] were deposited extensively in the retina, choroid, and sclera at 3 weeks after the FD plus CXL treatment. Our data also showed that there was some AGE deposition in the sclera of FD myopic eyes, consistent with the mild increase in IOP in the FD eyes. Our study also showed that sCD44, MMP-2, and TIMP-2, which are reported to be upregulated in human glaucomatous eyes,[44–47] were increased in the aqueous humor or the scleral tissues, at different levels, in eyes of the FD group and FD plus CXL group. sCD44 is elevated in the aqueous humor of primary open-angle glaucoma (POAG) versus non-POAG eyes,[48–50] and its concentration correlates with the extent of visual field loss in POAG.[51] In our study, sCD44 increased significantly in the eyes of both the FD group and the FD plus CXL group. However, the increment of sCD44 in FD plus CXL eyes was significantly greater than that in FD eyes, which was consistent with the different increments of IOP in these two groups. MMPs and TIMPs are involved in POAG pathogenesis by impairing extracellular matrix turnover in the trabecular meshwork. Interestingly, the FD eyes showed a higher MMP-2/TIMP-2 ratio than did the FD plus CXL eyes, indicating that CXL can cause further TIMP-2 upregulation in FD eyes. This finding is similar to the imbalanced increase among MMPs and TIMPs, with a shift toward raised TIMP levels, found in human glaucomatous aqueous humor samples.[46–47,52,53] These manifestations supported the hypothesis that, although IOP was elevated in both the FD and the FD plus CXL eyes, increased scleral stiffness in myopic eyes may cause further damage and subsequent molecular biological changes leading toward glaucomatous pathology.

Although the exact mechanism remains unknown, the outflow reduction in the anterior chamber, tested by trypan blue staining, and the imbalanced MMP-2/TIMP-2 ratio indicated that extracellular matrix composition might be

involved in the pathology. Deduction of scleral expansion ability, which may lead to higher pressure absorption by the lamina cribrosa and cause damage to the optic nerve head, may not be the only explanation for glaucomatous changes in the FD plus CXL eyes. The deposition of AGEs in the retina, choroid, and sclera; increased expression of sCD44 in the aqueous humor; and increased expression of MMP-2 and TIMP-2 in the scleral tissue suggest that CXL can cause extensive changes in FD myopic guinea pig eyes.

The present study demonstrated that CXL may cause IOP increase and subsequent changes in optic disc, anterior segment, and sclera, along with inhibiting myopic progression and axial elongation in FD guinea pigs. Caution should be exercised when extrapolating these conclusions to humans because there are anatomical differences between guinea pigs and human beings. Although rodent models have been developed for many ocular diseases, including myopia and glaucoma,[54,55] some rodents do not have a non-collagenous lamina cribrosa.[56] The guinea pig has a lamina cribrosa, but its structure is not well studied. The guinea pig retina is essentially avascular. Moreover, human sclera, comparatively, is more cross-linked than rodents.[10] It is unknown if additional stiffening of the sclera, induced by CXL, can cause clinically relevant glaucomatous changes in human myopic eyes. Although CXL has not been clinically used on human myopic eyes to slow axial elongation and myopic progression, posterior scleral reinforcement (PSR) has been applied in clinics ever since 1930. Xue et al.[57] reported modified PSR by using genipin cross-linked donor sclera on 40 young patients with high myopia. They found that six patients had 5 mm Hg or higher IOP than the fellow eye within the first week after surgery but all values were below 25 mm Hg. The average IOP for the surgery group was 17.4 $\pm$ 3.8 mm Hg, and it was 15.9 $\pm$ 2.8 mm Hg for the fellow eyes. IOP returned to normal without medication before discharge from the hospital (1 week in hospital). Another study evaluated the efficacy and safety of a novel PSR device for myopia suppression in 12 rabbit eyes and reported slightly transient IOP elevation at postoperative 1 week and 1 month.[58] These changes may not be clinically relevant in the short-term follow-up periods but do highlight the changes in IOP in scleral reinforcement treatment strategies. Moreover, PSR may not affect the recipient's lamina cribrosa directly, as scleral cross-linking does.

There are other limitations in this study. General anesthesia is required during the multiple genipin injections and OCT examination, so we used 4-week-old guinea pigs for the experiment because of the high mortality of anesthesia in 3-week-old guinea pigs, which are commonly used in the other studies.[7–9] Additionally, due to the lack of large-scale studies of guinea pig optic discs by OCT, the standard OCT parameters of normal guinea pig optic discs are not available. Moreover, comprehensive studies should be performed to observe the histological and molecular changes in the anterior and posterior segments of the CXL plus FD eyes. Further studies are warranted to investigate the long-term efficacy and safety issue of scleral CXL in myopic eyes.

In conclusion, this is the first report, to the best of our knowledge, regarding CXL effects on optic disc parameters in a guinea pig myopia model with FD. CXL causes increased IOP and subsequent optic disc, anterior segment, and scleral changes while inhibiting myopic progression and axis elongation in FD guinea pig eyes. Therefore, applying CXL to control myopia raises safety concerns.

Acknowledgments

Supported by Shenyang Science and Technology Planning project (21-173-9-24).

The pathology and molecular biology part of the experiment was guided by Professor Keyan Chen of Animal Laboratory of China Medical University.

Disclosure: **L. Guo**, None; **R. Hua**, None; **X. Zhang**, None; **T.Y. Yan**, None; **Y. Tong**, None; **X. Zhao**, None; **S.C. Chen**, None; **M. Wang**, None; **N.M. Bressler**, None; **J. Kong**, None

References

1. Morgan IG, Ohno-Matsui K, Saw SM. Myopia. *Lancet*. 2012;379:1739–1748.
2. Ohno-Matsui K, Lai TY, Lai CC, Cheung CMG. Updates of pathologic myopia. *Prog Retin Eye Res*. 2016;52:156–187.
3. McMonnies CW. An examination of the relation between intraocular pressure, fundal stretching and myopic pathology. *Clin Exp Optom*. 2016;99:113–119.
4. Huang W, Duan A, Qi Y. Posterior scleral reinforcement to prevent progression of high myopia. *Asia Pac J Ophthalmol (Phila)*. 2019;8:366–370.
5. Zhu S-Q, Zheng L-Y, Pan A-P, Yu A-Y, Wang Q-M, Xue A-Q. The efficacy and safety of posterior scleral reinforcement using genipin cross-linked sclera for macular detachment and retinoschisis in highly myopic eyes. *Br J Ophthalmol*. 2016;100:1470–1475.
6. Momose A. Long-term results of scleral reinforcement surgery. *Am J Ophthalmol*. 1987;104:554–555.
7. Wang M, Corpuz CC. Effects of scleral cross-linking using genipin on the process of form-deprivation myopia in the guinea pig: a randomized controlled experimental study. *BMC Ophthalmol*. 2015;15:89.
8. Liu S, Li S, Wang B, et al. Scleral cross-linking using riboflavin UVA irradiation for the prevention of myopia progression in a guinea pig model: blocked axial extension and altered scleral microstructure. *PLoS One*. 2016;11:e0165792.
9. Wang Y, Han Q, Han F, Chu Y, Zhao K. Experimental study of glyceraldehyde cross-linking of posterior scleral on FDM in guinea pigs. *Zhonghua Yan Ke Za Zhi*. 2014;50:51–59.
10. Kimball EC, Nguyen C, Steinhart MR, et al. Experimental scleral cross-linking increases glaucoma damage in a mouse model. *Exp Eye Res*. 2014;128:129–140.
11. Clayson K, Pan X, Pavlatos E, et al. Corneoscleral stiffening increases IOP spike magnitudes during rapid microvolumetric change in the eye. *Exp Eye Res*. 2017;165:29–34.
12. Hannon BG, Luna C, Feola AJ, et al. Assessment of visual and retinal function following in vivo genipin-induced scleral crosslinking. *Transl Vis Sci Technol*. 2020;9:8.
13. Ostrin LA, Wildsoet CF. Optic nerve head and intraocular pressure in the guinea pig eye. *Exp Eye Res*. 2016;146:7–16.
14. Howlett MH, McFadden SA. Form-deprivation myopia in the guinea pig (*Cavia porcellus*). *Vision Res*. 2006;46:267–283.
15. Guofu C, Jibo Z, Fan L. Changes in intraocular pressure during form-deprivation and the recovery period in the guinea pig. *Chinese J Optom Ophthalmol Vis Sci*. 2009;11:81–88.
16. Coudrillier B, Tian J, Alexander S, Myers KM, Quigley HA, Nguyen TD. Biomechanics of the human posterior sclera: age- and glaucoma-related changes measured using inflation testing. *Invest Ophthalmol Vis Sci*. 2012;53:1714–1728.

17. An G, Omodaka K, Hashimoto K, et al. Glaucoma diagnosis with machine learning based on optical coherence tomography and color fundus images. *J Healthc Eng.* 2019;2019:4061313.
18. Hua R, Gangwani R, Guo L, et al. Detection of preperimetric glaucoma using Bruch membrane opening, neural canal and posterior pole asymmetry analysis of optical coherence tomography. *Sci Rep*. 2016;6:21743.
19. Rao HL, Pradhan ZS, Suh MH, Moghimi S, Mansouri K, Weinreb RN. Optical coherence tomography angiography in glaucoma. *J Glaucoma.* 2020;29:312–321.
20. Jnawali A, Beach KM, Ostrin LA. In vivo imaging of the retina, choroid, and optic nerve head in guinea pigs. *Curr Eye Res.* 2018;43:1006–1018.
21. Ostrin LA, Wildsoet CF. Optic nerve head and intraocular pressure in the guinea pig eye. *Exp Eye Res*. 2016;146:7–16.
22. Pérez-Merino P, Velasco-Ocana M, Martinez-Enriquez E, Revuelta L, McFadden SA, Marcos S. Three-dimensional OCT based guinea pig eye model: relating morphology and optics. *Biomed Opt Express*. 2017;8:2173–2184.
23. Strouthidis NG, Girard MJ. Altering the way the optic nerve head responds to intraocular pressure-a potential approach to glaucoma therapy. *Curr Opin Pharmacol.* 2013;13:83–89.
24. Quigley HA, Addicks EM, Green WR, Maumenee AE. Optic nerve damage in human glaucoma. II. The site of injury and susceptibility to damage. *Arch Ophthalmol.* 1981;99:635–649.
25. Quigley HA, Hohman RM, Addicks EM, Massof RW, Green WR. Morphologic changes in the lamina cribrosa correlated with neural loss in open-angle glaucoma. *Am J Ophthalmol.* 1983;95:673–691.
26. Norman RE, Flanagan JG, Sigal IA, Rausch SMK, Tertinegg I, Ethier CR. Finite element modeling of the human sclera: influence on optic nerve head biomechanics and connections with glaucoma. *Exp Eye Res.* 2011;93:4–12.
27. Levy NS, Crapps EE. Displacement of optic nerve head in response to short-term intraocular pressure elevation in human eyes. *Arch Ophthalmol*. 1984;102:782–786.
28. Zeimer RC, Ogura Y. The relation between glaucomatous damage and optic nerve head mechanical compliance. *Arch Ophthalmol*. 1989;107:1232–1234.
29. Yan DB, Coloma FM, Metheetrairut A, Trope GE, Heathcote JG, Ethier CR. Deformation of the lamina cribrosa by elevated intraocular pressure. *Br J Ophthalmol*. 1994;78:643–648.
30. Bellezza AJ, Rintalan CJ, Thompson HW, Downs JC, Hart RT, Burgoyne CF. Deformation of the lamina cribrosa and anterior scleral canal wall in early experimental glaucoma. *Invest Ophthalmol Vis Sci*. 2003;44:623–637.
31. Bellezza AJ, Rintalan CJ, Thompson HW, Downs JC, Hart RT, Burgoyne CF. Anterior scleral canal geometry in pressurised (IOP 10) and non-pressurised (IOP 0) normal monkey eyes. *Br J Ophthalmol.* 2003;87:1284–1290.
32. Yang H, Downs JC, Sigal IA, Roberts MD, Thompson H, Burgoyne CF. Deformation of the normal monkey optic nerve head connective tissue after acute IOP elevation within 3-D histomorphometric reconstructions. *Invest Ophthalmol Vis Sci*. 2009;50:5785–5799.
33. Roberts MD, Liang Y, Sigal IA, et al. Correlation between local stress and strain and lamina cribrosa connective tissue volume fraction in normal monkey eyes. *Invest Ophthalmol Vis Sci*. 2010;51:295–307.
34. Coudrillier B, Tian J, Alexander S, Myers KM, Quigley HA, Nguyen TD. Biomechanics of the human posterior sclera: age- and glaucoma-related changes measured using inflation testing. *Invest Ophthalmol Vis Sci*. 2012;53:1714–1728.
35. Girard MJ, Suh JK, Bottlang M, Burgoyne CF, Downs JC. Scleral biomechanics in the aging monkey eye. *Invest Ophthalmol Vis Sci*. 2009;50:5226–5237.
36. Fazio MA, Grytz R, Morris JS, et al. Age-related changes in human peripapillary scleral strain. *Biomech Model Mechanobiol.* 2014;13:551–563.
37. Girard MJ, Downs JC, Burgoyne CF, Suh J-KF. Experimental surface strain mapping of porcine peripapillary sclera due to elevations of intraocular pressure. *J Biomech Eng.* 2008;130:041017.
38. Sigal IA, Flanagan JG, Ethier CR. Factors influencing optic nerve head biomechanics. *Invest Ophthalmol Vis Sci*. 2005;46:4189–4199.
39. Burgoyne CF, Downs JC, Bellezza AJ, Suh J-KF, Hart RT. The optic nerve head as a biomechanical structure: a new paradigm for understanding the role of IOP-related stress and strain in the pathophysiology of glaucomatous optic nerve head damage. *Prog Retin Eye Res*. 2005;24:39–73.
40. Sigal IA, Yang H, Roberts MD, et al. IOP-induced lamina cribrosa deformation and scleral canal expansion: Independent or related? *Invest Ophthalmol Vis Sci*. 2011;52:9023–9032.
41. Schweitzer C, Cougnard-Gregoire A, Rigalleau V, et al. Autofluorescence of skin advanced glycation end products as a risk factor for open angle glaucoma: the ALIENOR study. *Invest Ophthalmol Vis Sci*. 2018;59(1):75–84.
42. Kandarakis SA, Piperi C, Topouzis F, Papavassiliou AG. Emerging role of advanced glycation-end products (AGEs) in the pathobiology of eye diseases. *Prog Retin Eye Res*. 2014;42:85–102.
43. Tezel G, Luo C, Yang X. Accelerated aging in glaucoma: immunohistochemical assessment of advanced glycation end products in the human retina and optic nerve head. *Invest Ophthalmol Vis Sci.* 2007;48:1201–1211.
44. Budak YU, Akdogan M, Huysal K. Aqueous humor level of sCD44 in patients with degenerative myopia and primary open-angle glaucoma. *BMC Res Notes.* 2009;2:224.
45. Giovingo M, Nolan M, McCarty R, et al. sCD44 overexpression increases intraocular pressure and aqueous outflow resistance. *Mol Vis*. 2013;19:2151–2164.
46. Ji ML, Jia J. Correlations of TIMP2 and TIMP3 gene polymorphisms with primary open-angle glaucoma. *Eur Rev Med Pharmacol Sci*. 2019;23:5542–5547.
47. Ashworth Briggs EL, Toh T, Eri R, Hewitt AW, Cook AL. TIMP1, TIMP2, and TIMP4 are increased in aqueous humor from primary open angle glaucoma patients. *Mol Vis*. 2015;21:1162–1172.
48. Chen S, Huang W, Wang J, et al. Soluble CD44 and vascular endothelial growth factor levels in patients with acute primary angle closure. *Acta Ophthalmol.* 2015;93:e261–e265.
49. Knepper PA, Miller AM, Choi J, et al. Hypophosphorylation of aqueous humor sCD44 and primary open-angle glaucoma. *Invest Ophthalmol Vis Sci*. 2005;46:2829–2837.
50. Nolan MJ, Koga T, Walker L, et al. sCD44 internalization in human trabecular meshwork cells. *Invest Ophthalmol Vis Sci*. 2013;54:592–601.
51. Nolan MJ, Giovingo MC, Miller AM, et al. Aqueous humor sCD44 concentration and visual field loss in primary open-angle glaucoma. *J Glaucoma.* 2007;16:419–429.
52. Määttä M, Tervahartiala T, Harju M, Airaksinen J, Autio-Harmainen H, Sorsa T. Matrix metalloproteinases and their tissue inhibitors in aqueous humor of patients with primary open-angle glaucoma, exfoliation syndrome, and exfoliation glaucoma. *J Glaucoma.* 2005;14:64–69.
53. Rönkkö S, Rekonen P, Kaarniranta K, Puustjärvi T, Teräsvirta M, Uusitalo H. Matrix metalloproteinases and their inhibitors in the chamber angle of normal eyes

Investigative Ophthalmology & Visual Science

and patients with primary open-angle glaucoma and exfoliation glaucoma. *Graefes Arch Clin Exp Ophthalmol.* 2007;245:697–704.

54. Morrison J, Farrell S, Johnson E, Deppmeier L, Moore CG, Grossmann E. Structure and composition of the rodent lamina cribrosa. *Exp Eye Res.* 1995;60:127–135.
55. Chen L, Zhao Y, Zhang H. Comparative anatomy of the trabecular meshwork, the optic nerve head and the inner retina in rodent and primate models used for glaucoma research. *Vision*. 2016;1:4.
56. May CA, Lütjen-Drecoll E. Morphology of the murine optic nerve. *Invest Ophthalmol Vis Sci.* 2002;43:2206–2212.
57. Xue A, Zheng L, Tan G, et al. Genipin-crosslinked donor sclera for posterior scleral contraction/reinforcement to fight progressive myopia. *Invest Ophthalmol Vis Sci*. 2018;59:3564–3573.
58. Yuan Y, Zong Y, Zheng Q, et al. The efficacy and safety of a novel posterior scleral reinforcement device in rabbits. *Mater Sci Eng C Mater Biol Appl.* 2016;62:233–241.